TRANSACTIONS OF THE INSTITUTE OF FLUID-FLOW MACHINERY

No. 134, 2016, 11–28

Paweł Bagiński*, Grzegorz Żywica

The influence of temperature on dynamics of the rotor – foil bearing system

Department of Turbine Dynamics and Diagnostics, Institute of Fluid Flow Machinery, Polish Academy of Sciences, 80-231 Gdańsk, Fiszera 14, Poland

Abstract

The paper presents the research on the effect of elevated temperature on the dynamic performance of a rotor supported by foil bearings. The tests were carried out on the test rig equipped with a module for increasing temperature around the bearings. A 3 kW motor with two ceramic ball bearings was connected to the shaft by means of a flexible coupling. The shaft was supported by gas foil bearings. The maximum rotational speed of the rotor was 24000 rpm. The tests were performed with the operating rotor, covering multiple start and stop cycles at room and elevated temperatures. During the first stage of experimental investigation vibration, displacement and temperature values for the two bearings were recorded. Then, the temperature was raised to approx. 200 °C within one of the bearing supports. The parameters mentioned above were registered and compared with the results obtained during room temperature operation. After each test bearings were disassembled, regenerated as necessary and reassembled. After analysis of the results achieved, it could be noted that the system was sensitive to the altering of operating conditions of the rotor. The elevated temperature around the shaft has increased its diameter, thereby reducing the lubricating gap. In spite of adverse operating conditions affecting the rotor, the whole system operated in a safe and stable manner.

Keywords: Foil bearings; Rotordynamics; Temperature distribution

1 Introduction

Modern fluid-flow machinery often contains severalfold bearings of different types, which cover the full range of potential operating conditions that may be encoun-

*Corresponding Author. Email adress: pbaginski@imp.gda.pl

tered. The most common bearings that are fit for universal use are rolling bearings. There is quite a number of different types of rolling bearings, e.g., steel, hybrid, ceramic, precision or high-speed ones. Their drawbacks are poor vibration damping capability and short service life. Another group of bearings widely used in many devices and machines are the hydrostatic and hydrodynamic slide bearings. They became very popular due to their ability to withstand heavy loads, very good vibration damping capability and long lifespan. From a practical point of view their main disadvantages are: fairly low rotational speeds, necessity to continually supply of a lubricant (usually oil) and purchase price. It should be noted that gas bearings have become increasingly popular in the last decade. These bearings can be divided into three basic groups. The first group is made up of externally pressurized gas-lubricated bearings (aerostatic bearings) which were used, among others, in a 3 kW microturbine that is a component of the cogeneration micro power plant [1], developed at the Szewalski Institute of Fluid Flow Machinery, Polish Academy of Science (IMP PAN). The second group of gas bearings are self-acting ones (aerodynamic bearings). However, they are rarely applied since they require highly precise manufacture and small lubricant film thickness which is very difficult to achieve. Another characteristic of aerodynamic bearings is their low load-carrying ability. The last group of gas bearings comprises foil bearings in which there is a structural interlayer between the shaft and the bush. Most often this is a set of metal foils with a thickness of about 0.1 mm. The foil that is in direct contact with the bearing journal, and on which the lubricating film that lifts up the shaft forms, is called top foil. The supporting foil, one might say, the foil pressing the top foil against a shaft is corrugated and is referred to as a bump foil.

The whole structure is a sophisticated and effective shaft vibration dampening system. It is considered as the greatest strength of a foil bearing and provides very useful feature – variable geometry of the lubricating gap. The first mentions of studies on foil bearings date back to the 1960s and 1970s [3]. In subsequent years gas foil bearings were investigated on the basis of measurements [4,5] and numerical analyses [6,7]. Some of the scientific studies were focused on the selection of foil materials in order to ensure long bearing life under the expected operating conditions [8,9], whereas the other research concerned bearing designs equipped with a structural interlayer [4,10]. Most often, static and/or dynamic experimental research were carried out on a single foil bearing [11]. A next evolutionary step in the development of foil bearings was their incorporation into oil-free turbomachines [12–14]. The outcomes of these experimental studies – conducted at the end of the 20th century – confirmed that bearings of this type have the poten-

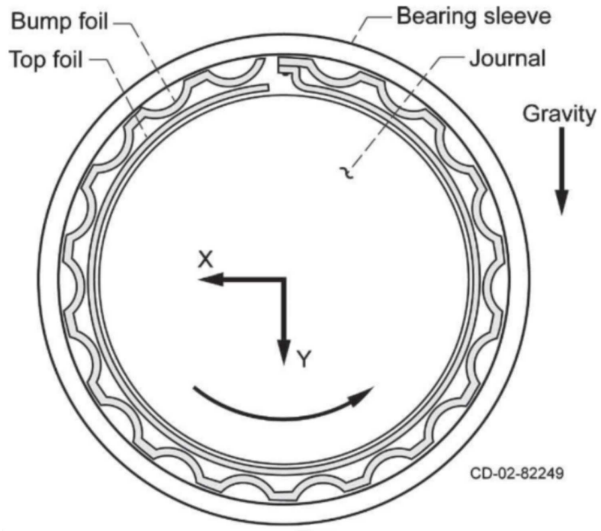

Figure 1: Typical journal foil bearing cross-section [2].

tial to be industrially viable. Nevertheless that has changed greatly over the last dozen years. Numerous papers have been published giving detailed descriptions of successive generations of foil bearings, new materials used in their construction as well as various industrial applications. Such rich sources of information permitted to push forward interesting ideas which were translated into specific technical solutions. One example of this is the application of microturbines fitted with foil bearings which are intended for use in an organic Rankine cycle (ORC) cogeneration system producing electricity and heat for the needs of a single-family house [15]. Insufficient lubricating properties of the working medium, a high rotational speed of the generator shaft and changing temperature (20–120 °C) were the main reasons that led the scientists to adopt such a solution. The test rig was built in order to thoroughly investigate the properties of custom-made foil bearings. It was designed to achieve high rotational speeds and elevated temperatures in the immediate vicinity of bearing supports, and also provides a hassle-free way to introduce the most frequently encountered defects in fluid-flow machinery (e.g., misalignment or unbalance). The research was designed to explore how the elevated ambient temperature affects the bearing operation and dynamics of the rotor – bearing system.

2 The test rig and research methodology

The experimental studies were carried out on the rigid rotor dynamics test rig equipped with a laboratory rotor supported by two foil bearings. Its photograph is shown in Fig. 1. The rotating system rests on the solid, steel plate which, along with its specially designed supporting structure, forms a sort of a 'table'. The supports for mounting bearings and sensors are fixed into place using screws. The rotor is actuated by a high-speed electrospindle via the coupling. The bearing supports consist of two parts enabling rapid exchange of the tested bearings. The heating devices, namely the heat gun and infrared illuminators, are located in the immediate vicinity of the bearing node no. 2. The heat gun is constructed of the heating pipe and duct fan. It discharges air at the desired temperature which heats up the rotating system. The air flow rate can be adjusted in addition to the outlet temperature. The hot air flow is pointed in the direction of the bearing node situated near the free end of the shaft (see Fig. 2).

The infrared illuminators make heating the shaft more efficient. The application of additional heating devices causes that the process of heating takes place at both sides of the bearing support no. 2. The diagram indicating the arrangement of heating devices is presented in Fig. 2. A detailed description of the devices that are component parts of the test rig described can be found in [2].
The measurement system was composed of the following elements: temperature and rotational speed sensors, accelerometers (for measurement of absolute vibrations of the bearing supports) and eddy current sensors (for measurement of relative shaft vibration). A portable, multichannel data acquisition system, LMS SCADAS Mobile analyzer, was employed during tests for measurements of dynamic performance of the operating machine and its temperature (using thermocouples). Additionally, a professional infrared camera, FLIR E50, was used to determine temperature distributions on the outer surfaces of the test rig's components.

Basic technical parameters of the test rig are as follows:

- maximum rotational speed: 24 000 rpm,
- nominal rotational speed: 18 000 rpm,
- shaft and bearing nominal diameters: 34 mm,
- diameter of the electrospindle shaft: 20 mm,
- steel plate dimensions: 1000×500×20 mm,
- number of bearing supports: 2,
- test rig weight: approx. 130 kg.

The tested bearings were developed within the framework of cooperation between the Szewalski Institute of Fluid-Flow Machinery and the Lodz University of Tech-

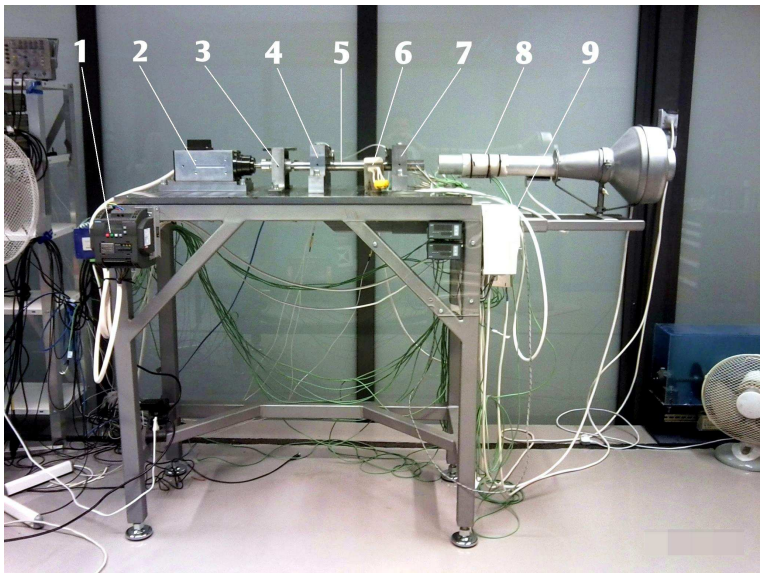

Figure 2: Rotor dynamics test rig – general view, without heat shield: 1 – speed controller, 2 – drive motor (electrospindle), 3 – coupling, 4 – bearing support no. 1, 5 – rotor shaft, 6 – infrared illuminators, 7 – bearing support no. 2, 8 – heat gun, 9 – temperature controller.

nology [16]. The arrangement of holes for thermocouple mounting in the bush and the fully assembled bearing are presented in Fig. 4. The grooves that are visible on the inner surface of the bush act as foil locks. The thermocouples were inserted through the grooves located on the outer surface of the bush.

The bearing is characterized by the following basic parameters:

- nominal diameter of the journal: 34 mm,
- outer diameter of the bush: 65 mm,
- bearing length: 40 mm,
- foil thickness: 0.1 mm,
- foil material: Inconel 625,
- type of the top foil coating: fluoropolymer based,
- type of the journal coating: made of chromium oxide (Cr_2O_3), plasma sprayed [16].

Previous experiements showed us that the method of fixing of thermocouples is crucial – not only for precision of measurement, but also for the proper functioning of a foil bearing [17]. Incorrect installation of thermocouples may lead to the damage of a sliding coating of the foil which reveals itself in a high and local

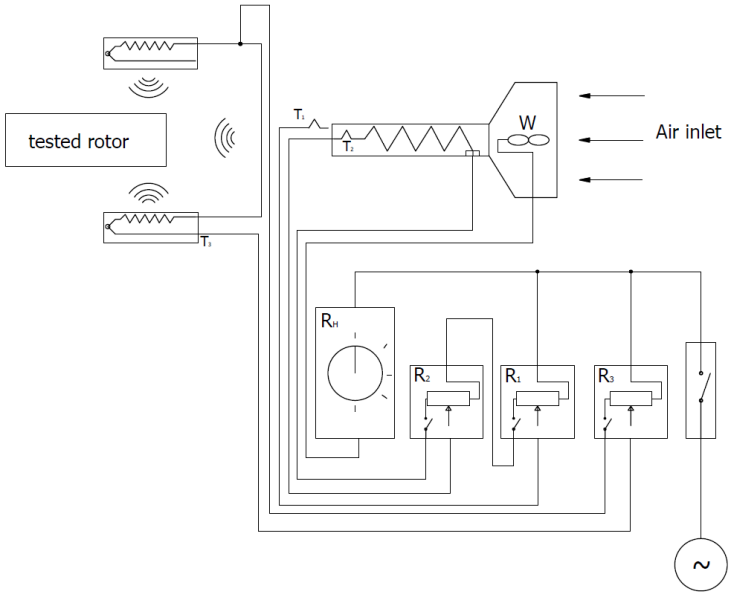

Figure 3: Diagram showing the arrangement of heating devices mounted on the test rig: T – thermocouple, W – fan, R_1–R_3 – controllers.

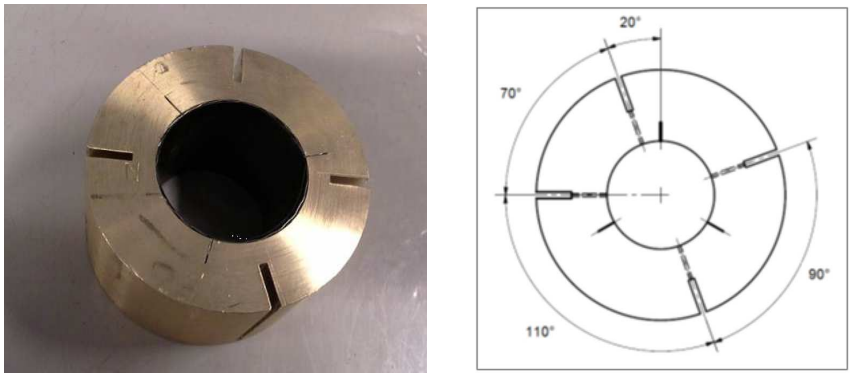

Figure 4: Photo of the bearing bush with the foil set fully installed (on the left side) and the arrangement of grooves for thermocouple mounting (on the right side). The nominal internal diameter is 34 mm.

increase of temperature and, consequently, permanent damage to the bearing [18,19]. The measurement of the temperature of the top foil was carried out using K-type thermocouples (the shielded measurement junctions of which have

a diameter of 1.0 mm). The thermocouples were inserted into the holes with diameters of 4 mm – previously drilled for this purpose – in such a way that their measurement junctions were in contact with the outer surface of the top foil. Thermocouple wires were routed through the wide grooves (milled to the specified dimension) which are visible on the outer surface of the sleeve (see Fig. 5). These wires were fixed in place by means of a high temperature resistant silicone sealant. The grooves and holes are located at the circumferential angular positions 20°, 100°, 200° and 290°, corresponding to the angle of rotor shaft rotation. Use of an appropriate number of temperature sensors allowed for the determination of a circumferential temperature distribution in the bearing. In each drilled hole three measurement junctions were put in three parallel directions, giving a total of 12 thermocouples for a single bearing (Fig. 5). This was the only thermocouples configuration for which the tests were carried out.

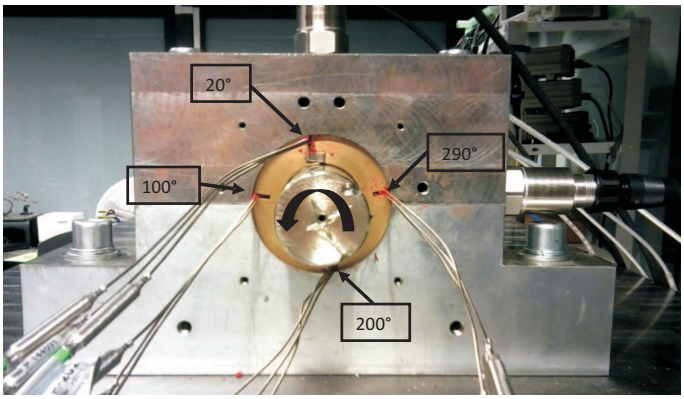

Figure 5: Bearing no. 2 located at the free end of the shaft. Four black arrows indicate the locations in which the thermocouples were inserted.

3 Research focusing on the system dynamics and bearing temperature

The research was conducted at the Machine Vibrodiagnostics Laboratory, located on the premises of the IMP PAN in Gdańsk. The measurements of vibration of the rotating system equipped with a rotor supported by aerodynamic foil bearings were carried out. The two step approach involved two sequential measurements, the first at room temperature immediately followed by the second at elevated temperature. During the measurement at an elevated temperature, the bearing node

no. 2 was heated using the available heating devices, as explained in more detail in the previous section. It was planned to achieve the bearing node temperature of about 150 °C, in view of the fact that temperatures of the same order of magnitude (and even higher) occur inside casings of power microturbines operating with low-boiling mediums. On the other hand, 200 °C was the upper temperature limit since the top foils' coatings had been put at a slightly higher temperature. Exceeding this temperature limit would be likely to cause melting of the sliding layer and bearing damage. The heat shield was used during the measurements performed at the elevated temperature. It was composed of several panes of glass, sealed with a high temperature resistant silicone. The heat shield has a two-part structure in which the dividing plane passes through the centerline of the shaft. The shield's openings are of such shape as to fit the shield to the rotor and allow the heat gun's outlet pipe and the thermocouples' wires to be inserted through these openings. The element described was used to keep the hot air in the immediate vicinity of the bearing node no. 2 and in this way to simulate the conditions typical for real devices. Figure 6 presents the bearing node no. 2 with the heat shield fully installed.

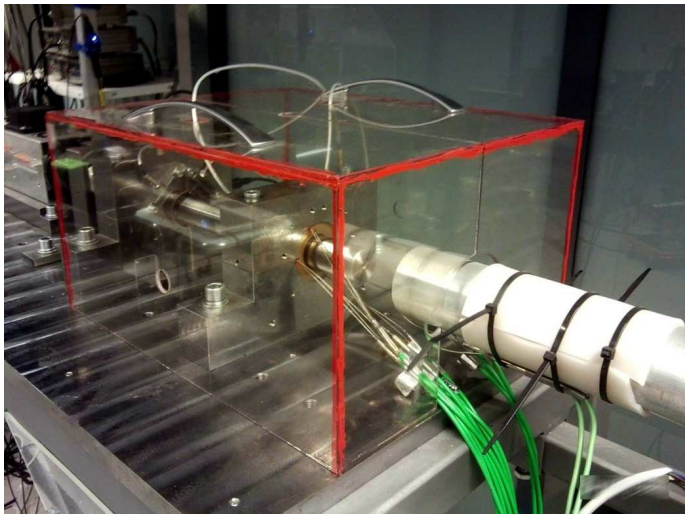

Figure 6: Bearing node no. 2 with the heat shield fully installed.

3.1 Measurement at room temperature

The first measurement was conducted at room temperature. The outcomes received at this stage were used, at a later stage, for the determination of the impact

of the elevated ambient temperature on the dynamic performance of the system tested. The measurement lasted 1906 s. The figures below illustrate the shaft relative vibration amplitudes as a function of time. Additionally, in each of these figures, a thick black line represents rotational speed of the rotor versus time. As

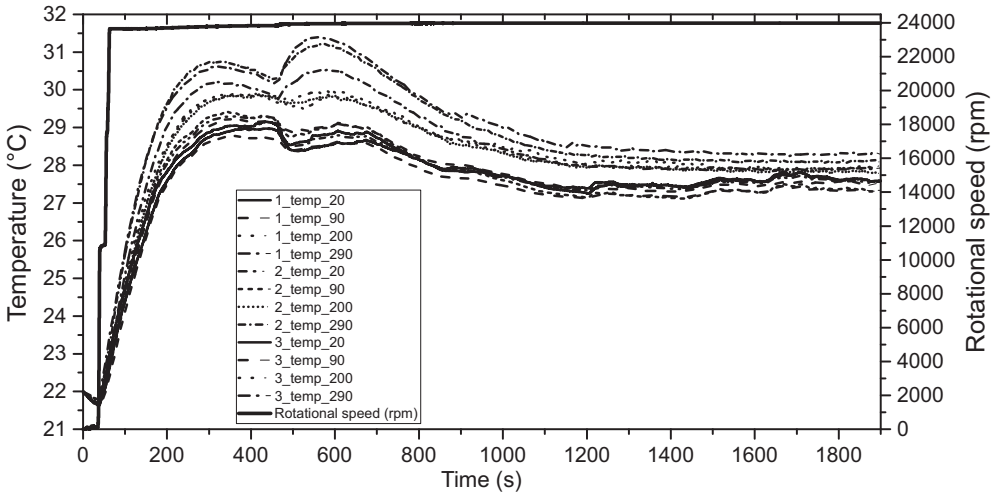

Figure 7: Temperatures of the bearing no. 2 during its operation at room temperature measured at various points in the bush vs. time (thick black line represents rotational speed of the rotor).

Fig. 7 shows, temperature of the bearing no. 2 has stabilized at around 26 °C (at the ambient temperature of 20 °C). The maximum temperature of the top foil was 29.5 °C. The top foil temperature increased by 8 °C during the first 300 s of the measurement. It peaked and entered its decline, stabilizing itself 1800 s. after the start of the measurement. The highest temperature values were recorded for the thermocouples located at the angular positions 200° and 290° (see Fig. 4) while the lowest values were obtained for the thermocouples placed at the two other angular positions, with temperature differences as small as ±0.5 °C. Approximately 450 s after the start of measurement, the rotating system faced a series of vibrations after which the bearings started to operate stably (i.e., the foil sets fitted into actual operating conditions resulting from the load and rotational speed of the rotor shaft), which brought about a change in temperature of the bearing no. 2. As can be seen in Fig. 7, the rotor initially operated at a slightly lower rotational speed than that assumed during the research planning phase. Following a series of vibrations observed, the eccentricity of bearing no. 1 decreased, reflecting the fact that the bearing capacity increased. The shaft in bearing no. 2 changed its

position but the vibration amplitude remained at the same level, i.e., 15–25 μm (Fig. 8). The increase in rotational speed to the assumed value of 24 000 rpm has reduced the shaft torque. This meant that air flow conditions in the bearing were optimal at the actual load and speed. The maximum relative vibration amplitudes for both bearings were 0.3 mm and 0.25 mm (Figs. 8 and 9, respectively), but the graphs were cut so as to better show the vibration values.

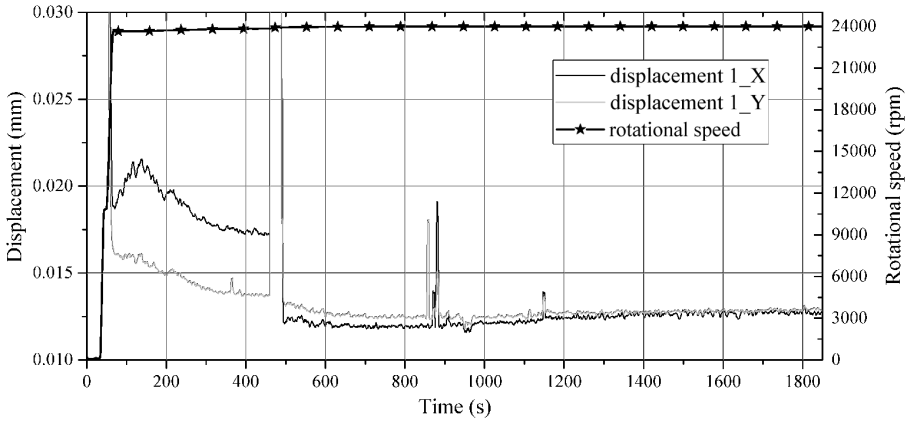

Figure 8: Relative vibration amplitudes of the shaft in bearing no. 1 vs. time.

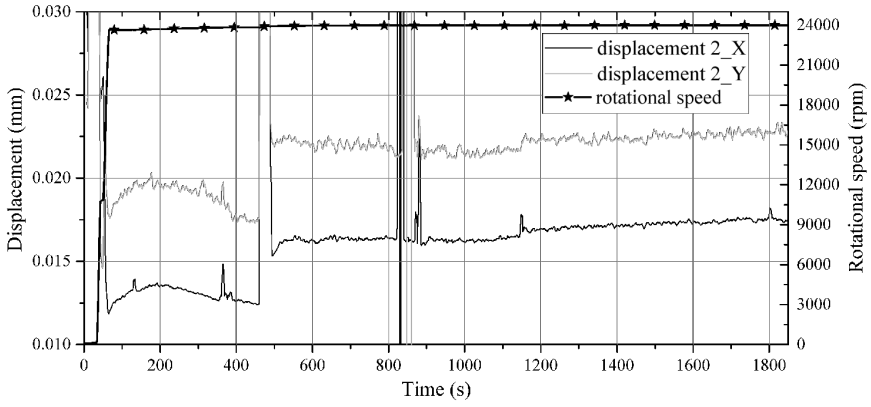

Figure 9: Relative vibration amplitudes of the shaft in bearing no. 2 vs. time.

The vibration trajectories had very low amplitudes. Having analyzed the graphs in Fig. 10 showing the vibration acceleration spectrums, can be easily identified main harmonic components (1X, 2X and 3X), which are a testament to the shaft misalignment. Moreover, 1/2-order subharmonics are present in both graphs. Technically, this would notably imply that there is a certain instability in the bearing operation. As, however, this instability did not lead to an uncontrolled increase in vibration, such a state of affairs could be deemed admissible.

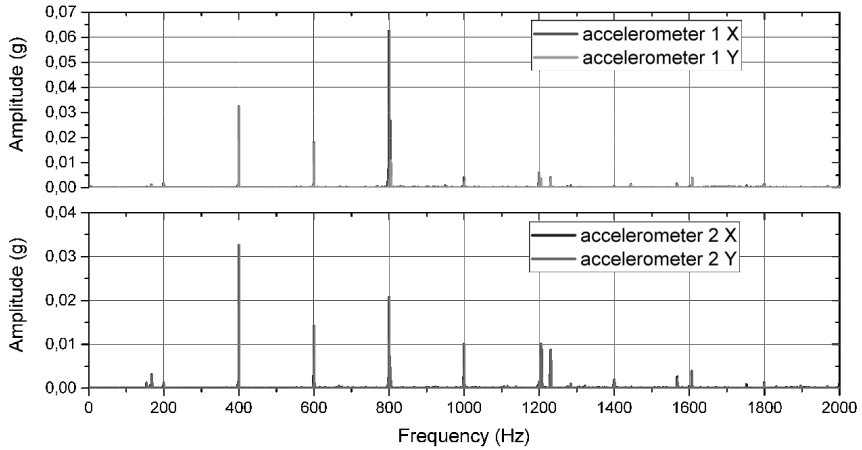

Figure 10: Spectrums showing absolute vibration accelerations registered after 1800 s from the start of measurement.

During the experimental investigation of the foil bearing operation, also the temperatures of the journal's antifriction layer were registered. Figures 11 and 12 present thermal images registered by means of the infrared camera. The bearings installed in the test rig were new; they needed breaking-in. Therefore, in the early phase of operation, the journal temperature in the bearing no. 1 exceeded 100 °C and in the bearing no. 2 reached 60 °C. After the bearing no. 1 broke in, it started to operate under a full-film lubrication regime (i.e., the foil set had situated itself properly and had got a right shape) and the journal temperature began to decrease till about 50 °C. This implied that there was an intense friction between the top foil and the journal. The heat generated in this way manifested itself in a locally observed rise in temperature. After the aerodynamic lubricating film started to prevent friction, the air at a temperature of approx. 20 °C was sucked in into the bearing, which caused a drop in the temperature of the journal. The temperature of the foil set in the bearing node no. 1 is not known since no measurements of its value were taken.

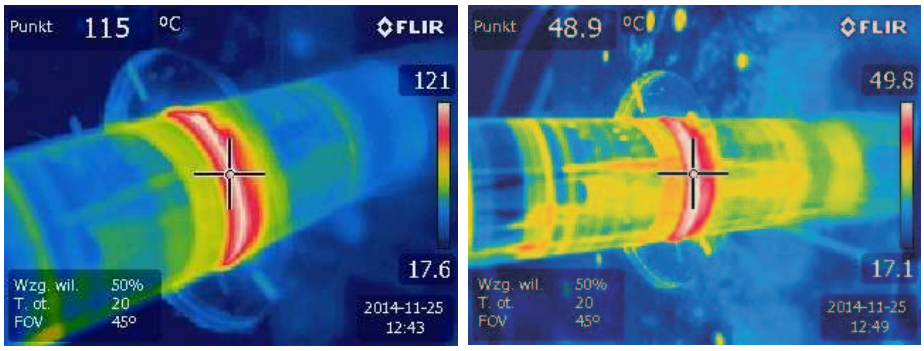

Figure 11: Temperatures of the outer surface of the bearing journal no. 1 registered at the beginning of the measurement (on the left side) and at the time when the bearing components operated under a full-film lubrication regime (on the right side).

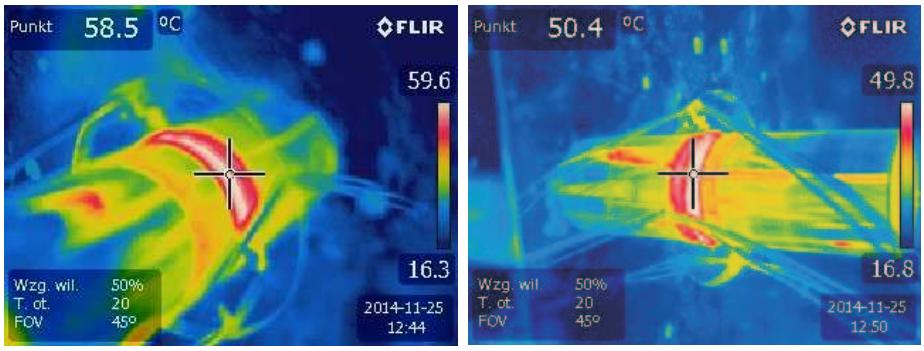

Figure 12: Temperatures of the outer surface of the bearing journal no. 2 registered at the beginning of the measurement (left image) and at the time when the bearing components operated under a full-film lubrication regime (right image).

In the bearing no. 2, the temperature of the shaft coating also went down to 50 °C in the last few minutes of the measurement carried out at room temperature. The temperature value of the top foil is derived by temperatures of the shaft and the air sucked in into the bearing.

3.2 Measurement at elevated temperature

This section describes the measurement performed under conditions in which a hot airstream was present in the immediate vicinity of a bearing node. For this purpose, the heat gun shown in Fig. 1 was employed. The free end of the shaft and bearing no. 2 were heated with direct hot air (having a temperature of 180 °C)

discharged by the heat gun. As a result, the increase of temperatures of the shaft itself and the bearing lubricant was achieved. During the first minutes of the measurement, the rotor operated at the nominal speed of the motor (18000 rpm) and at room temperature. After approx. 5 min. of operation, the heating system was turned on (see a vertical black line in Fig. 13). During the measurements, there was a temporary heating system failure, what can be seen in the graph showing the temperatures of the top foil in bearing no. 2 measured at several points in the bush as a function of time (temporary fall in temperature between 1500 and 2000 s, Fig. 13). Figures 14 and 15 present shaft relative vibration displacements and amplitudes registered for the bearings no. 1 and no. 2, respectively. Additionally, Figs. 13–15 contain the black line representing the rotor's rotational speed as a function of time. Figure 16 shows the vibration acceleration spectra obtained after 6000 s from the start of measurement.

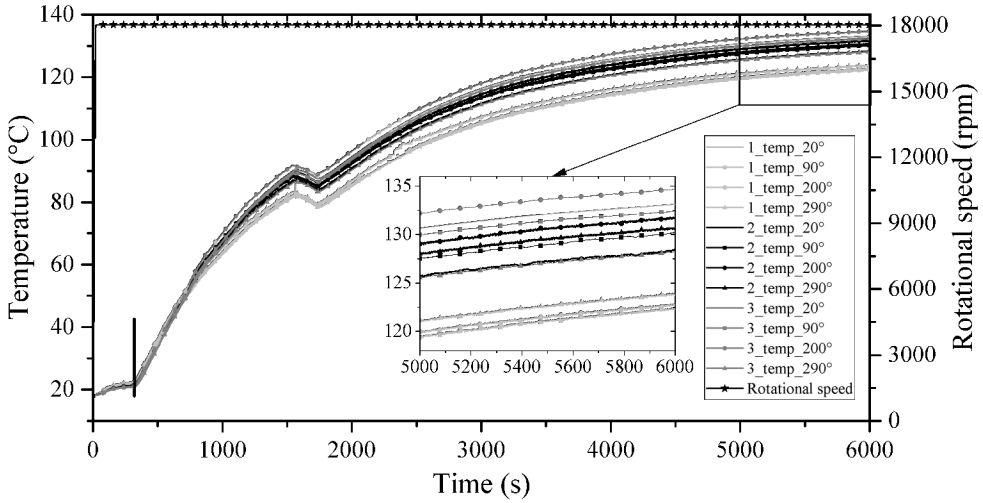

Figure 13: Temperatures of the bearing no. 2 during its operation at elevated temperature measured at various points in the bush vs. time (thick black line represents rotational speed of the rotor).

As Fig. 13 shows, there have been substantial changes in the foil set temperature, but most importantly, the whole heating process ran smoothly and was consistent with the assumptions. The maximum temperatures were recorded in the upper part of the bush (angular position 20°) from the hot air flow side (approx. 139 °C) and at the angular position 200° (137 °C). The lowest temperatures were registered for the thermocouples located at the angular positions 290° (unlike for the rotor operation at room temperature) and 100°, i.e., around 127 °C and

134 °C, respectively. During the time of measurement, the thermocouple marked with '290_2' (placed at the angular position 290°) started malfunctioning periodically and the one marked '200_3' (angular position 200°, located at the hot air flow side) got damaged. The interruption in heating needed to replace the fuse in the control system has entailed the temperature drops of approx. 4 °C. Not surprisingly, the highest temperatures were recorded from the heat gun side (thermocouples marked 'angle_3'), whereas the thermocouples located from the infrared illuminators side (marked 'angle_1') were the ones with the lowest temperatures. The temperatures inside the bush differed significantly from each other, but the ones registered by the thermocouples marked angle_1 and angle_2 had similar values. The heating of the rotating system caused the increase of journal eccentricity in the lubricating gap and higher vibration amplitudes ranging between 10 μm and 20 μm, depending on the bearing concerned (see Figs. 14 and Fig. 15). These values are slightly lower than the ones obtained during the first measurement, since the rotor operated at lower rotational speed. In the figures, it is also clearly visible that the rotor dynamics depends on the ambient temperature – this is particularly evident when the heating devices were turned off. During the heating process, the rotor's diameter has been expanding over time. Having analyzed the upper graph in Fig. 14 (see the line marked 'displacement 1_X' representing the shaft relative displacement in the X direction which was registered for the bearing no. 1), you can easily notice that the shaft was in direct contact with the foils or even with the outer surface of the bush.

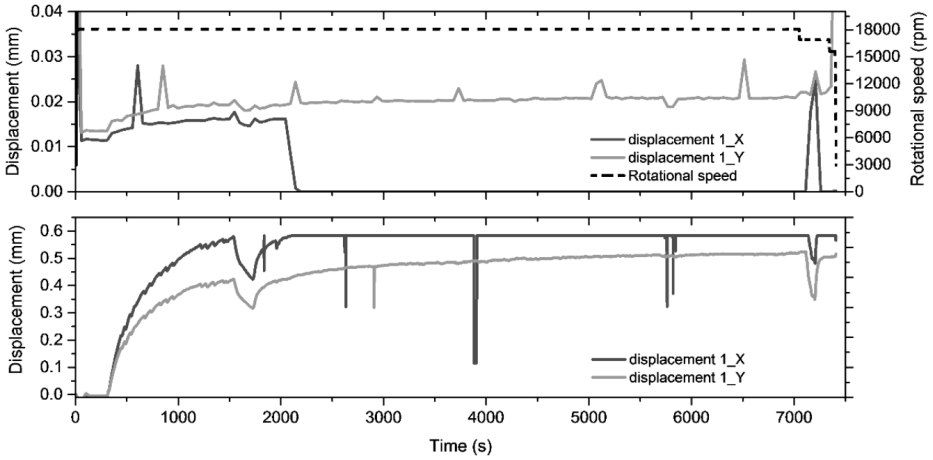

Figure 14: Shaft relative vibration displacements (upper graph) and amplitudes (lower graph) registered for the bearing no. 1 during its operation at elevated temperature.

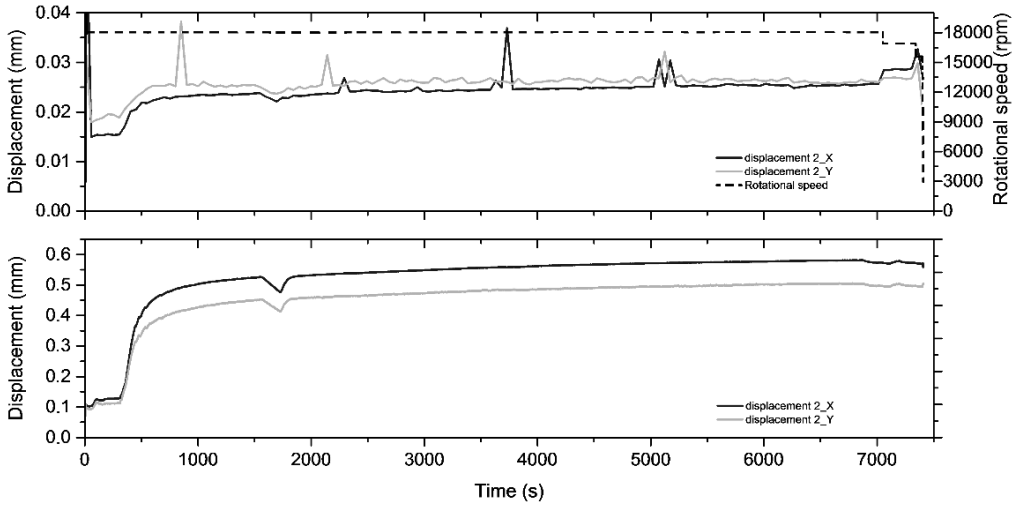

Figure 15: Shaft relative vibration displacements (upper graph) and amplitudes (lower graph) registered for the bearing no. 2 during its operation at elevated temperature.

The vibration accelerations spectra contain the main harmonic components (1X, 2X, ...) and the presence of the 1/2-order subharmonic has almost completely ceased to be visible. During the experiment, a number of elevated vibration levels – which took place with a certain degree of regularity over a lengthy period – were observed. One of the possible causes was the operation of the heating devices control system.

In order to be sure that this is the cause of the phenomenon observed, a series of manual impulse tests was conducted, consisting in hitting the particular components of the test rig. These tests confirmed that the excitation originates from the place in which the heating controls are situated. It was spotted that the regularity of the elevated vibration levels was caused by the operation of the thermostat's contact and its on/off switching while carrying out the manual impulse tests. The vibration measurements were taken during the run-up and run-down of the rotor, at both room and elevated temperatures. Figure 17 presents the shaft relative vibration amplitudes registered during the run-up of the rotor. The upper graph in this figure shows the results obtained during the system operation at room temperature (approx. 20 °C) and the lower graph presents the results measured when the bearing no. 2 operated at the elevated temperature (up to approx. 140 °C). In particular, it can be observed that the critical speed of the rotor (i.e. 7774 rpm which corresponds to 129.57 Hz) recorded during the second mea-

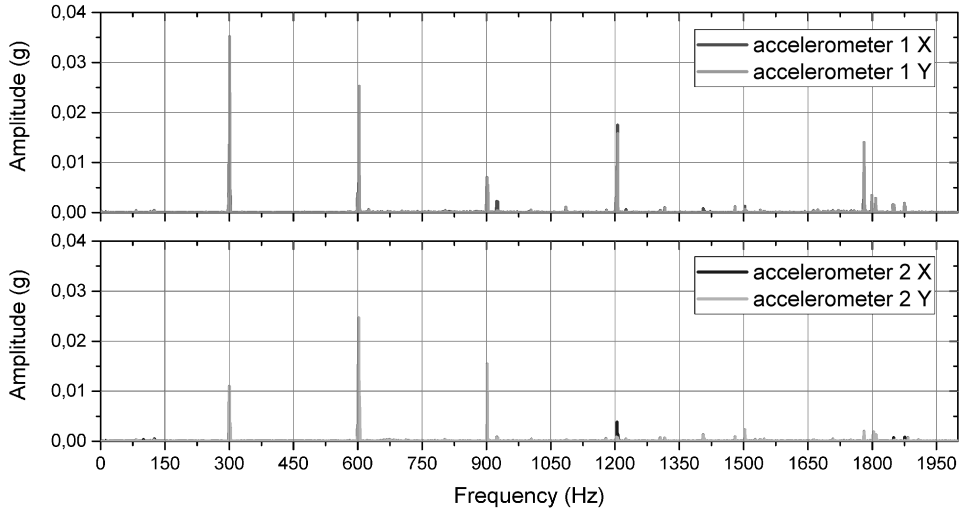

Figure 16: Vibration acceleration spectra registered after 6000 s from the start of measurement.

surement conducted at elevated temperature is significantly lower as compared to the first measurement – where it amounted to 8427 rpm or, in other words, 140.45 Hz). This is due to a substantial decrease in stiffness of the bearing's structural layer made of thin foils under the action of hot a airstream.

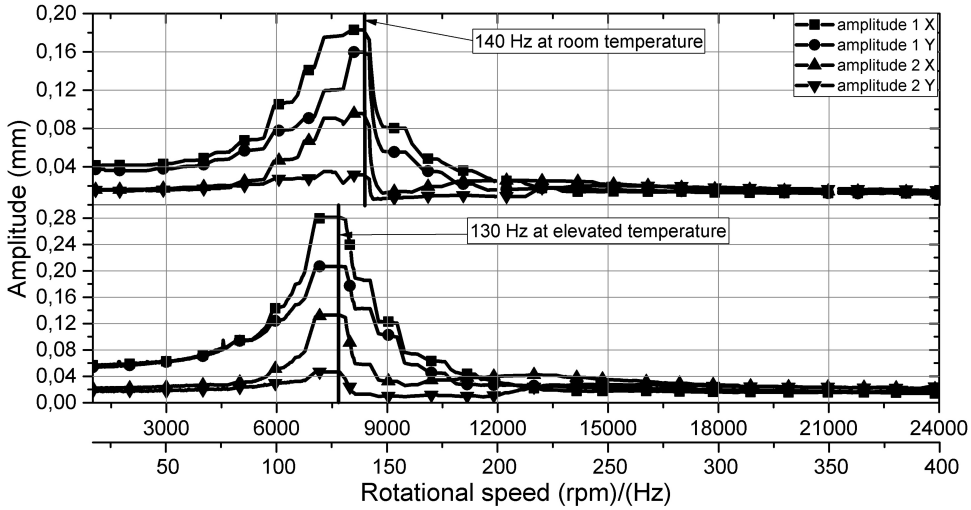

Figure 17: Shaft relative vibration amplitudes registered during run-up of the rotor, carried out at both room and elevated temperatures (upper and lower graph, respectively).

4 Summary and conclusions

The aim of this work was to determine the effect of ambient temperature on dynamics of the rotor supported by foil bearings. The comparison between the measurement results obtained at room and elevated temperatures was made. The experimental tests used the heating devices (the heat gun and infrared illuminators) accompanied by a heat shield reducing heat losses in the immediate vicinity of the bearing no. 2. The bearings have been running stably and smoothly at the highest ambient temperatures (130–140 °C). Despite the operation at such large temperatures, there has been no significant impact on the rotor dynamics. Although an increase in the shaft eccentricity and vibration amplitudes has been observed as a result of the measurement taken, it is considered that they are admissible in the speed and temperature range investigated and can be explained primarily by the existence of thermal expansion changing the qualities of the constituent materials of the bearing. The authors of the paper take the view that high variations in temperature within the bearing have no material impact on its operation. These temperature differences were no greater than 12 °C. This is, at least in part, the result of applying the heat shield, inside of which the temperature had a more even distribution. Initially, the bearings were characterized by high instability of operation since the temperature inside the bearings was increasing (the journal diameter was also increasing). When the bearing temperature stabilised itself, the bearings started to operate properly. Such an ability to adapt to operating conditions is a unique characteristic of foil bearings. On the basis of the analyses performed, it can be presumed that a foil bearing operating in a real machine does not generate additional heat (i.e. the heat that could adversely affect the proper functioning) if the aerodynamic lubricating film is already fully formed. Thermocouples the measurement junctions of which have diameters of 1.0 mm have proven easy to install and appropriately durable; it seems, however, that their response time is too long.

Received in July 2016

References

[1] Żywica G., Kiciński J., Kaczmarczyk T.Z., Ihnatowicz E., Turzyński T., Bykuć S.: *Prototype of the domestic CHP ORC system: Construction and experimental research.* In: Proc. 3rd Int. Sem. on ORC Power Systems, ASME ORC 2015, Brussels, Oct. 12–14, 2015.

[2] Howard S.A., San Andrés L.: *A new analysis tool assessment for rotordynamic modeling of gas foil bearings.* J. Eng. Gas Turbines Power **133**(2011), 022505-9.

[3] Ma J.T., Pirvics J., Rightmire G.K., Bosma R.: *Discussion*. J. Lubr. Technol. Trans. ASME **92**(1972), 4, 220–222.

[4] Agrawal G.L.: *Foil air/gas bearing technology-an overview*. ASME Pap. 97-GT, 1997, 347.

[5] Müftü S., Kaiser D.J.: *Measurements and theoretical predictions of head/tape spacing over a flat-head*. Tribol. Int. **33**(2000), 5, 415–430.

[6] Braun M.J., Choy F.K., Dzodzo M., Hsu J.: *Two-dimensional dynamic simulation of a continuous foil bearings.pdf*. Tribol. Int. **29**(1996),29, 61–68.

[7] Żywica G., Kiciński J.: *The numerical analysis of the steam microturbine rotor supported on foil bearings*. Adv. Vib. Eng. **11**(2012), 2, 113–120.

[8] Laskowski J.A., DellaCorte C.: *Friction and wear characteristics of candidate foil bearing materials from 25°C to 800°C*. Lubr. Eng. **52**(1996), 605–616.

[9] Hashimoto H.: *Experimental study of porous foil bearings for web-handling*. Tribol. Int. **33**(2000), 3-4, 191–196.

[10] Sudheer Kumar Reddy D., Swarnamani S., Prabhu B.S.: *Analysis of aerodynamic multileaf foil journal bearings*. Wear **209**(1997), 1-2, 115–122.

[11] Dellacorte C.: *A new foil air bearing test rig for use to 700°C and 70000 rpm*. Tribol. Trans. **41**(1998), 3, 335–340.

[12] Lian-You Xiong, Gang Wu, Chun-Zheng, Yan-Zhong Li: *A feasibility study on the use of new gas foil hearings in cryogenic turboexpander*. Adv. Cryogenic Eng. **43**(1998), 661–665.

[13] Howard S.A.: *Rotordynamics and Design Methods of an Oil – Free Turbocharger*. Tribology Trans. **42**(1999), 1, 174–179.

[14] DellaCorte C., Lukaszewicz V., Valco M.J., Radil K.C., Heshmat H.: *Performance and durability of high temperature foil air bearings for oil-free turbomachinery*. Tribology Trans. **43**(2000), 4, 774–780.

[15] Kiciński J.: *New ideas in distributed cogeneration and power engineering new energy policy of the European Union related to the civil energy generation*. Transactions IFFM **127**(2015), 7–25.

[16] Kozanecki Z., Łagodziński J., Miazga K.: *Development of manufacturing technology and research gas foil bearings*. Internal Rap. IMP PŁ I10/501/12/34/2013, Łódź 2014 (in Polish).

[17] Żywica G., Bagiński P. Banaszek, S.: *Experimental studies on foil bearing with a sliding coating made of synthetic material*. J. Tribol. **138**(2015), 1, 011301.

[18] Kiciński J., Żywica G., Bagiński P., Niewiadomski J.: *Experimental development of a method of gas foil bearings under conditions conducive to the occurrence of thermal instability*. Internal Rap. IMP PAN 987/2013, Gdansk 2013 (in Polish).

[19] Żywica G., Banaszek S., Bagiński P.: *Initial tests of the foil bearings test rig in configuration with two bearing supports. Measurements of vibration trajectories of the journals and vibration acceleration amplitudes of the bearing journals*. Internal Rap. IMP PAN 180/2014, Gdansk 2014 (in Polish).